Proceedings World Geothermal Congress 2020+1
Reykjavik, Iceland, April - October 2021

The Interaction of the Plate Boundary Movement in 2020 and Exploitation of Geothermal Fields on the Reykjanes Peninsula, Iceland

Ólafur G. Flóvenz, Vincent Drouin, Kristján Ágústsson, Egill Árni Guðnason, Gylfi Páll Hersir, Thorbjörg Ágústsdóttir and Ingvar Þór Magnússon

ÍSOR – Iceland GeoSurvey, Grensásvegi 9, 108, Reykjavík, Iceland

ogf@isor.is, www.isor.is

Claus Milkereit, Torsten Dahm and Philippe Jousset

Helmholtz Centre Potsdam GFZ German Research Centre for Geosciences, Potsdam, Germany

Keywords: seismic swarms, uplift, geothermal, Reykjanes Peninsula, Iceland

ABSTRACT

January 22nd, 2020 an intense earthquake swarm started just east of the Svartsengi geothermal field on the Reykjanes Peninsula in SW-Iceland. Simultaneously, a rapid uplift started in the middle of the geothermal field centred close to the re-injection wells of the Svartsengi power plant. The seismic activity was strongly episodic, and during the following months it spread over a large proportion of the plate boundary along the Reykjanes Peninsula. There are indications that the original seismicity might have been triggered by the pressure increase at the source of uplift underneath the geothermal field. The vertical displacement consisted of three periods of uplift from January to July separated by periods of subsidence. Since Mid-July 2020, continuous subsidence has been ongoing. The character of the seismic activity is typical for the classical plate movements along the plate boundary of the peninsula, where oblique rift prevails while the cause of the uplift is debated. Possible explanations are three magmatic intrusions forming narrow and thin sills at shallow depth below the geothermal field, fluid expansion and contraction phenomena beneath the re-injection wells or a mixture of both effects. An intrusion of mantle CO_2 is also a candidate. Our evaluation of the available data does not prove or disprove any of the hypotheses on the origin of the pressure and volume increase at the source of the uplift. In future modelling we consider important to account for the high temperature, pressure, and permeability at the source of uplift and possible interaction between magma, carbon dioxide and the in-situ geothermal fluid.

1. INTRODUCTION

The Svartsengi power plant is located within the Eldvörp branch of the Svartsengi volcanic system on the Reykjanes Peninsula in SW Iceland. It was commissioned in 1976 to produce hot water for a district heating system in nearby communities, including the Keflavik International Airport. It is now operated by the power company HS Orka (https://www.hsorka.is/en/). The power plant is now the heart of a Resource Park including the Blue Lagoon, one of the most popular tourist sites in Iceland as well as a few industrial entities that utilize the valuable resource stream from the power plant (Albertsson and Jónsson, 1976). The average annual production in 2019 was 238 L/s (7,000,000 Tn/y) of 240°C hot fluid corresponding to 19,034 TJ of primary energy (Orkustofnun, 2020) and installed electrical power is 76,4 MW. About ⅔ of the produced fluid is re-injected (De Freitas, 2018) but it is variable. The district heating system now serves approximately 25.000 people.

The location of the Svartsengi power plant on roughly 800 years old lava within a volcanic fissure swarm is of concern as eruptions might endanger the whole Resource Park and cut off the hot- and cold-water supply for the whole area. Therefore, it was alarming, when an intensive earthquake swarm connected to a local uplift started in January 2020 and kept on for more than half a year. This paper describes these events and discusses possible causes of the uplift.

2. GEOLOGICAL BACKGROUND

The boundary separating the American and the Eurasian plate runs along the Reykjanes Peninsula (Fig.1) and is delineated by 5 to 10 km wide zone of seismic activity. It connects the central axis of the Reykjanes Ridge in the west to the Hengill triple junction in the east. The plate boundary (N70°E) is oblique to the spreading direction (N104°E) (e.g., Einarsson, 2008, Björnsson et al., 2020). Apart from the seismicity it is characterized by NE striking volcanic fissure systems and fracture zones superimposed on the seismic zone and N-S trending strike slip fissures formed in earthquakes. Both the seismicity and the volcanic activity are episodic but with very different frequency.

The episodic seismicity seems to occur approximately every 20-40 years (Björnsson et al., 2020) as intensive swarms that seem to cover the entire peninsula during a few years with maximum earthquake magnitude of about 6. Quieter intervals are in-between the active episodes but with locally persistent micro-seismicity. Source mechanisms of the larger earthquakes (M_L>3) typically give N-S trending right-lateral faults with less obvious traces in the surface geology. The persistent micro-seismicity shows, however, a variety of source mechanisms with a mixture of strike-slip, reverse and normal faulting (Kristjánsdóttir, 2011).

During postglacial times, the volcanic and related rifting episodes have occurred at 800-1000 years interval. Each of the three latest episodes did last for a few centuries and appear to start in the east and jump stepwise westwards with spacing of 100-200 years (Sæmundsson et al., 2020). The bulk of the volcanic activity occurs along the NE trending fissure swarms, mainly within the seismic zone, and extends from there several km towards NE along the associated fissure swarms (Fig.1) (Hjartarson and

Sæmundsson, 2014, Sæmundsson et al., 2016, http://jardfraedikort.is/). Beyond the eruptive part, the related faults and fissures extend far toward NE to NNE into the older crust, possibly underlain by dykes. This process is suggested to control the formation of the extensive and powerful low temperature fields in the older crust near Reykjavík and farther to the NNE (Sæmundsson et al., 2020).

The seismic crustal structure of the Reykjanes Peninsula has been the topic of several papers (Pálmason, 1971, Flóvenz, 1980, Weir et al., 2001, Kristjánsdóttir, 2013, Blanck et al., 2020). According to these studies, the depth to the lower crust (oceanic layer 3) is close to 4.5 km along the seismic zone from Reykjanes to Lake Kleifarvatn and the depth to Moho is about 15 km. It should be noted here that the Moho beneath Iceland is atypical; it is mostly derived from wide angel PmP reflections and an estimate of the density of the lower crust is closer to sub-Moho values that are normally found in oceanic crust (Kaban et al., 2002, White et al., 2001, Weir et al., 2001). The oceanic layer 3 is generally considered to be of 100% intrusions.

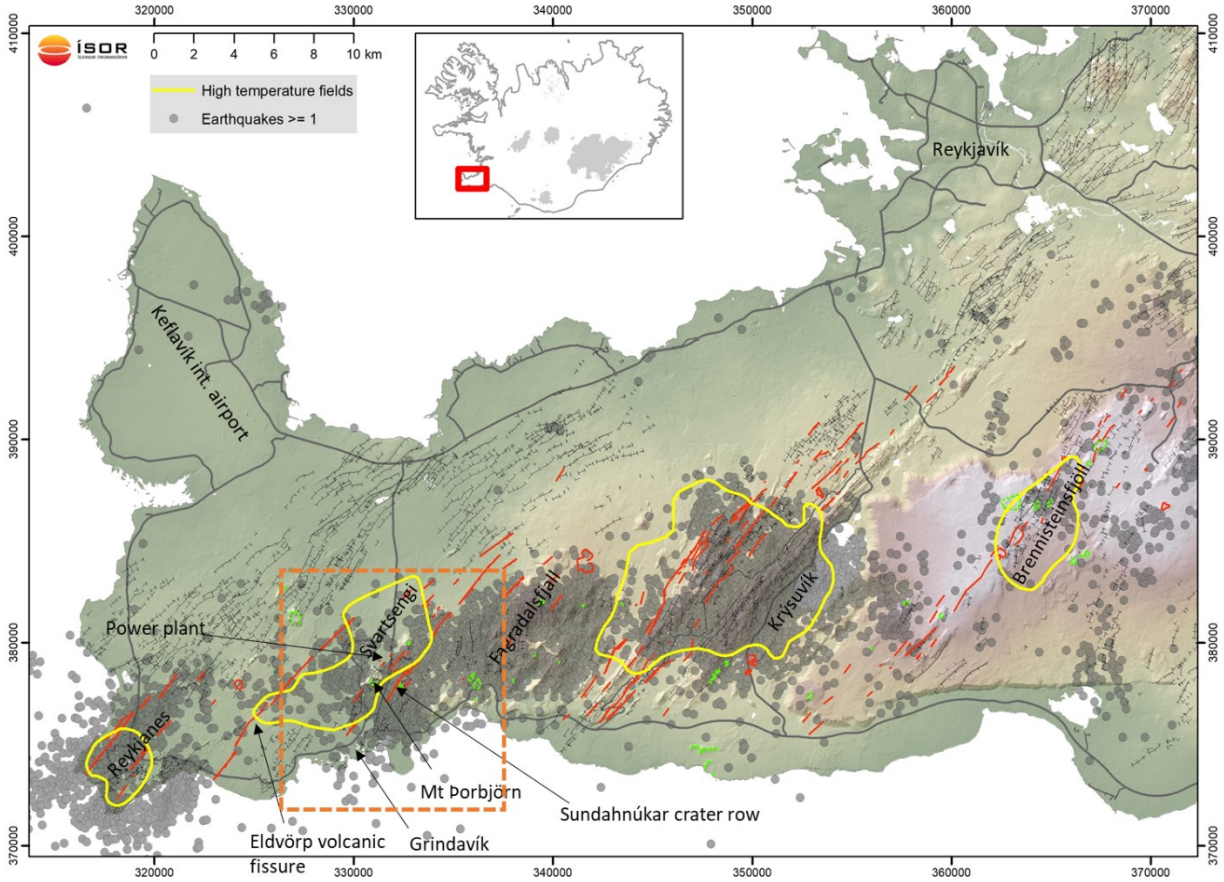

Figure 1: Map of faults, fissures, craters, and volcanic fissures on the Reykjanes Peninsula based on Sæmundsson et al. (2016). Red lines are postglacial volcanic eruption sites and craters from the ice age are green. The yellow lines outline the high temperature systems along the peninsula at approximately 1 km depth based on resistivity soundings. The grey dots are earthquakes larger than 1.0 M_L recorded by IMO since 1995. The absence of earthquakes around the production area of the Svartsengi power plant is notable. The faint shades of landscape in the background show many elongated NE-SW striking hyaloclastite ridges that were formed in eruptions during the last ice age. The orange dashed box shows the area used for more detailed analysis of the seismicity and the uplift in this paper.

Weir et al. (2001) report also a normal Vp/Vs value of 1.78 in their long-range refraction profile along the seismic zone of the Reykjanes Peninsula that indicates "that there is no significant fraction of distributed melt and that temperatures are below the solidus in the regions of crust sampled." This indication is supported by results of co-located MT/TEM resistivity soundings that have been carried out along the seismic zone as a part of geothermal exploration (Hersir et al., 2020, and Karlsdóttir et al., 2020). The results do not show clear signs of a similar deep seated highly conductive layer as exists beneath the axial volcanic rift-zones of Iceland nor a body conductive enough that it could be caused by molten material. The only indication is in Krýsuvík where a conductive body having an estimated volume of 1 km^3 was found at a depth of around 2 km below the central part of the high-temperature area. "This body coincides horizontally with the centre of an inflation source at 4–5 km depth, an uplift exceeding 50 mm/year in 2010. It has been suggested that the 2007–2016 inflation/deflation periods are linked to gas flux, as no signs of S-wave attenuation have been found. It is therefore unlikely that the deep-seated conductive body resolved by our resistivity models comprises partial melt" (Hersir et al., 2020). The general conclusion is that there is no evidence for molten material in the crust under the seismic zone of the Reykjanes Peninsula. However, this does not exclude very localized small pockets of magma intrusions, especially within the lower crust as the resolution of the seismic and resistivity data reduces with depth.

Four high temperature geothermal fields have developed on the peninsula (Reykjanes, Svartsengi, Krýsuvík and Brennisteinsfjöll) as shown on Figure 1. They are all located at the intersection of the postglacial volcanism and the seismic zone. Like in other high temperature systems in Iceland, their heat source is generally considered to be cooling intrusions at a few kilometres depth. The

reservoir temperature in these systems is 240-330°C based on temperature measurements in 1-3 km deep wells (De Freitas, 2018). One well, IDDP-2 in the Reykjanes high temperature field, has been drilled to 4.6 km depth (Friðleifsson et al., 2020) where bottom hole temperature is estimated to be around 600°C (Bali et al., 2020).

In Iceland, the earthquakes usually terminate sharply at a certain depth at each site defining the brittle-ductile (B/D) boundary of the crust. This boundary has been defined as the surface above which 95% of hypocentres occur and is clearly temperature dependent. Ágústsson and Flóvenz (2005) estimated the temperature at the B/D boundary beneath Iceland to be 745 ± 95°C. In case of the Reykjanes high temperature field the B/D boundary is approximately at 5.5 – 6.0 km depth (Blanck et al., 2020, Friðleifsson et al., 2020) or 1-1.5 km beneath the bottom of well IDDP-2. Therefore, the B/D boundary is likely at 600-700°C. Detailed analysis of the B/D boundary below the seismic zone on the Reykjanes Peninsula shows the B/D boundary at 6-7 km depth doming up to 4-5 km depth below the high temperature fields of Reykjanes and Krýsuvík (Blanck et al, 2020, Kristjánsdóttir, 2013). Outside the seismic zone, the temperature development with depth can be extrapolated from heat flow data in wells that are sufficiently far away from the hydrothermal system to represent background crustal heat flow. There exist five 500-1000 m deep wells on the northern part of the peninsula that are not disturbed by fluid flow beneath 300 m depth and can be used to calculate the crustal heat flow. By using temperature logging from these wells (Friðleifsson et al. 2002) we can calculate the temperature gradient in these wells to be 90-120°C/km, and by downward extrapolation to 650°C this gives the depth to the B/D boundary of 6-8 km which is consistent with the B/D depth at the flanks of the seismically active zone.

3. THE SVARTSENGI GEOTHERMAL FIELD

This paper mainly focuses on the area around the Svartsengi geothermal field, due to the centre of uplift being located within the field. The Svartsengi volcanic system is subdivided into the Eldvörp branch and the Svartsengi branch (Sæmundsson and Sigurgeirsson, 2013) as shown in Figure 2a.

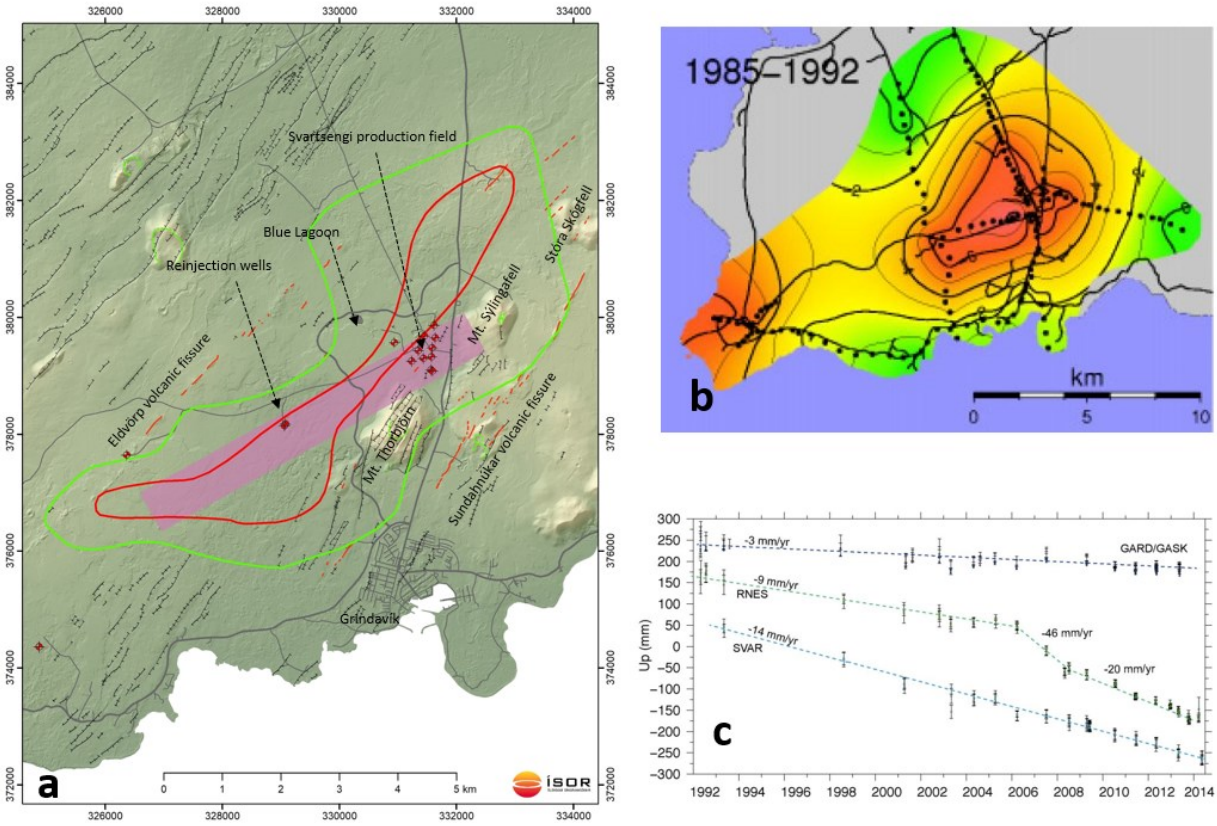

Figure 2: a) The depth to the top of the resistive core beneath Svartsengi (from Karlsdóttir, 1998) which marks the outline of the geothermal field as defined by the chlorite -epidote alteration zone. The location of selected wells is also shown together with location of faults (black lines) and volcanic fissures (red lines). The pink rectangle shows approximately the location of the suggested intrusion that could explain the uplift pattern (Michelle Parks, pers.com.) and is used in this paper to estimate the gravity effect of the three intrusions combined into a single one. b) A map of the subsidence caused by pressure drawdown due to geothermal production in Svartsengi. Measured by in levelling surveys (f. From Eysteinsson, 2000). c) Elevation changes in Svartsengi and Reykjanes from the beginning of production at each field until 2014 from Axelsson et al., (2015). The pink rectangle shows approximately the location of the suggested intrusion that could explain the uplift pattern (Michelle Parks, pers.com.) and is used in this paper to estimate the gravity effect of the three intrusions combined into a single one.

These volcanic systems are separated by a hyaloclastite mountain chain including Mt. Thorbjörn, Mt. Sýlingafell and Mt. Stóra-Skógfell, with the Eldvörp branch to the west and the Svartsengi branch to the east (Sæmundsson et al., 2016). The last eruption in the Eldvörp branch occurred in the early 13th century and the lava covers the area of the Svartsengi Resource Park (Sæmundsson

and Sigurgeirsson, 2013). The youngest eruption in the Svartsengi branch is 2400 years old. It formed the Sundahnúkar crater row (Sæmundsson and Sigurgeirsson, 2013) and produced the lava flow where the town of Grindavík is partly located.

The Svartsengi geothermal field was originally mapped by Schlumberger resistivity soundings in the early seventies (Pálmason, 2005). Later, TEM resistivity soundings were used to define the areal extent of the system (Karlsdóttir, 1998) (Fig 2 a). The resistivity soundings show clearly that Eldvörp and Svartsengi are a part of the same geothermal field, mostly striking NE-SW but changes to a E-W direction close to Eldvörp.

The production in Svartsengi started in 1976 and has been ongoing since. The production has caused large pressure reduction within the geothermal reservoir and has led to continuous land subsidence (Fig.2). The shape of the subsidence has been similar all the time. The shape of the subsidence anomaly looks like the shape of the geothermal field as outlined by the resistivity measurements in Figure 2a, albeit the shape of the land elevation changes is somewhat suffered by poor data density. Both datasets show a superposition of a NNE striking feature, similar to the strike of the regional volcanic fissures and E-W striking feature that coincides with the plate boundary and the main trend direction of the seismic zone of the Reykjanes Peninsula.

The subsurface of the Svartsengi production field has been analysed by use of well cuttings and well logging (Franzson, 1983, 1990). The uppermost 1100 m consist mostly of sequences of hyaloclastite formed in eruptions under ice separated by basaltic lavas from interglacial periods. Intrusions are observed below 700-800 m depth. The ratio of intrusions is <50% down to 1100 m where a zone of horizontal intrusions (sills) is found and reaches almost 90% of the rock to 1200 m depth. Farther down the ratio of intrusions is generally much less than 50%, at least to 1900 m depth. Altogether, six separate hyaloclastite layers are found down to 1100 m that has roughly been formed during the past 0.6 m.y. (Franzson, 1990).

4. THE START AND DEVELOPMENT OF THE 2020 UNREST PERIOD

Just before 14 UTC on January 22nd, 2020 an earthquake swarm started roughly 2 km east of the Svartsengi power plant beneath the Sundahnúkar eruption fissure (Figure 2a). The swarm was located by the national seismological network of the Icelandic Meteorological Office (IMO). Almost simultaneously, and later confirmed by InSAR data from the Sentinel-1 satellite, continuous GPS stations operated by the Institute of Earth Sciences of the University of Iceland (IES) showed that the land surface started to rise beneath the centre of the geothermal field, with maximum uplift close to the re-injection site. The uplift was assumed to be caused by a magmatic intrusion into the root of the geothermal system. An alternative explanation of fluid related phenomenon in the geothermal system was also suggested. These events created high attention of the scientific community and the Department of Civil Protection and Emergency Management in Iceland, as well as HS Orka and the local community. In response, IMO increased its monitoring, but IMO is responsible "for monitoring, analysing, interpreting, informing, giving advice and counsel, providing warnings and forecasts and, where possible, predicting natural processes and natural hazards" (www.vedur.is). Additional GPS stations were installed, the seismic network was improved by restoring abandoned stations and connecting on-line several local seismic stations operated by ÍSOR on behalf of the Czech Academy of Sciences (CAS). Several additional seismic stations were installed, both by GFZ in Potsdam in cooperation with ÍSOR, as well as the University of Cambridge in cooperation with the University of Iceland and ÍSOR. GFZ also installed continuous recording of strain in the optical fibre optic cable that lies from Reykjanes through Svartsengi to Grindavík in cooperation with Mila telecommunication company and ÍSOR and did several other measurements. ÍSOR measured gravity at permanent sites and monitored the uplift through InSAR data. HS Orka did monitor possible changes in gas composition of the geothermal fluid as well as the pressure in the reservoir. IMO monitored the chemical composition in fumaroles.

5. THE UPLIFT AS SEEN BY IN-SAR DATA

Interferometric Synthetic Aperture Radar (InSAR) is a technique that allows to observe surface deformation over large areas. The Sentinel-1 SAR mission acquires images over Reykjanes every 6 days with an ascending track (T16) and a descending track (T155). The T16 images are acquired 2.5 days later than the T155 images. We processed all acquisitions between 12 Dec. 2019 and 15 Nov. 2020. Deformation time-series were obtained by using the SBAS approach (Berardino et al., 2002). Interferograms were generated using the Interferometric synthetic aperture radar Scientific Computing Environment (ISCE2) while the SBAS inversion was done using an in-house software. We obtained two line-of-sight deformation time-series, one for each track. Their signals were then decomposed to extract the vertical deformation time-series, called near-Up to show the process approximations (Drouin & Sigmundsson, 2019).

The near-Up time-series show a clear inflation pattern, about 14 km long and 12 km wide, centred about 1 km west of Mt. Thorbjörn, for a total uplift of over 12 cm (Figure 3). When looking at the time-series in more detail, three inflation episodes can be observed, each followed by a deflation (Figure 4). All inflation patterns and spatial distributions are similar, indicating that it is likely to be the same source behind all these deformation episodes. The first inflation lasted for approximately 24 days and had a maximum uplift of about 6 cm. The second inflation lasted for approximately 48 days and had also a maximum uplift of about 6 cm. The third inflation lasted for 60 days and had a maximum uplift of 4 cm. Therefore, the uplift rate for the first inflation was about twice the one of the second inflation and four times the one of the third inflation. The first deflation lasted for approximately 24 days and had a maximum subsidence of about 10 mm, but this value is very uncertain because of the snow cover during this episode. The second deflation lasted also for approximately 24 days and a maximum subsidence of over 15 mm. The third deflation was still on-going as of 15 Nov., three months after it started subsiding. A M_L 3.4 earthquake happened on 18 July north of Mt. Thorbjörn and was associated with a local subsidence (grey area on Figure 4f). The broader subsidence pattern shows a maximum subsidence of over 25 mm.

The uplift is most likely caused by sudden pressure increase and corresponding volume expansion at certain depth beneath the centre of the uplifted area which is slightly west of Mt. Thorbjörn, close to the re-injection wells of the Svartsengi power plant. A Mogi model of the source indicates a depth of approximately 4.5 km beneath the centre of the geothermal field as defined by resistivity soundings (Fig. 2). The slightly elliptic form of the uplift anomaly is elongated along the direction of the resistivity anomaly suggesting the source to be of similar geometry and to follow the main strike of the high temperature field. This has been

modelled to fit to three magmatic intrusions at 3.2, 3.8 and 4.3 km depth with 95% confidence limits of 2.2 – 6.0 km (Michelle Parks pers. com.).

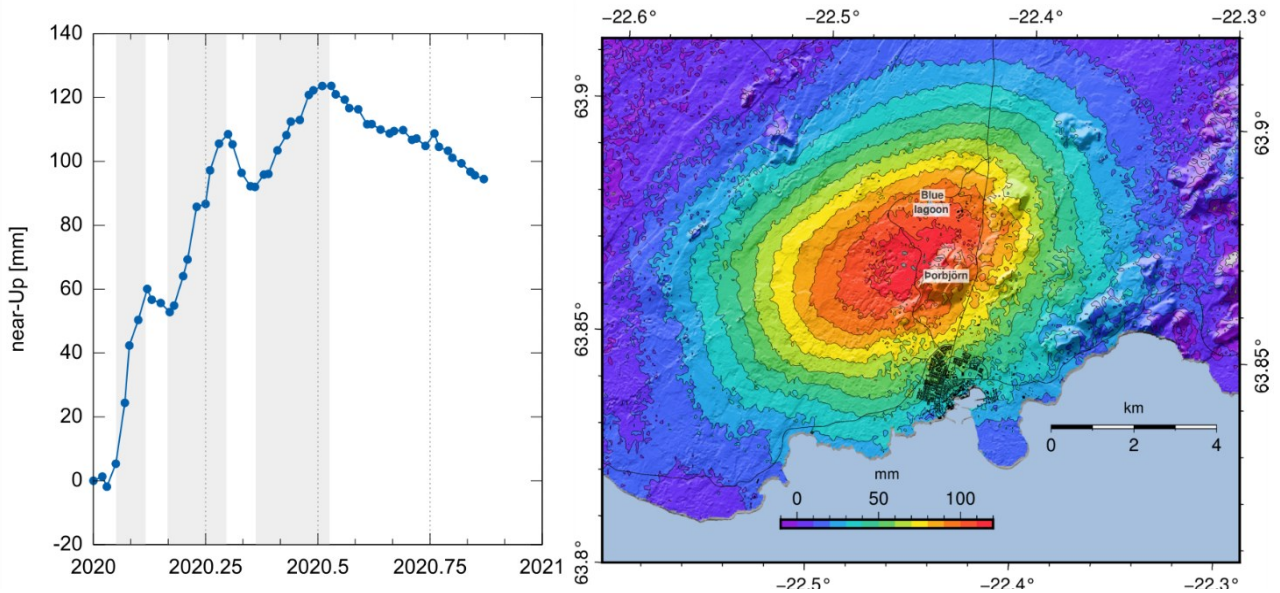

Figure 3: (Left) Time series of the near-Up displacement at the centre of maximum inflation. X-axis indicates time in decimal years. Gray areas show periods of inflation. (Right) Total inflation between the 19 January and the 11 July. Background shows shaded topography, buildings (black areas), roads (black lines), and ocean (grey/blue areas).

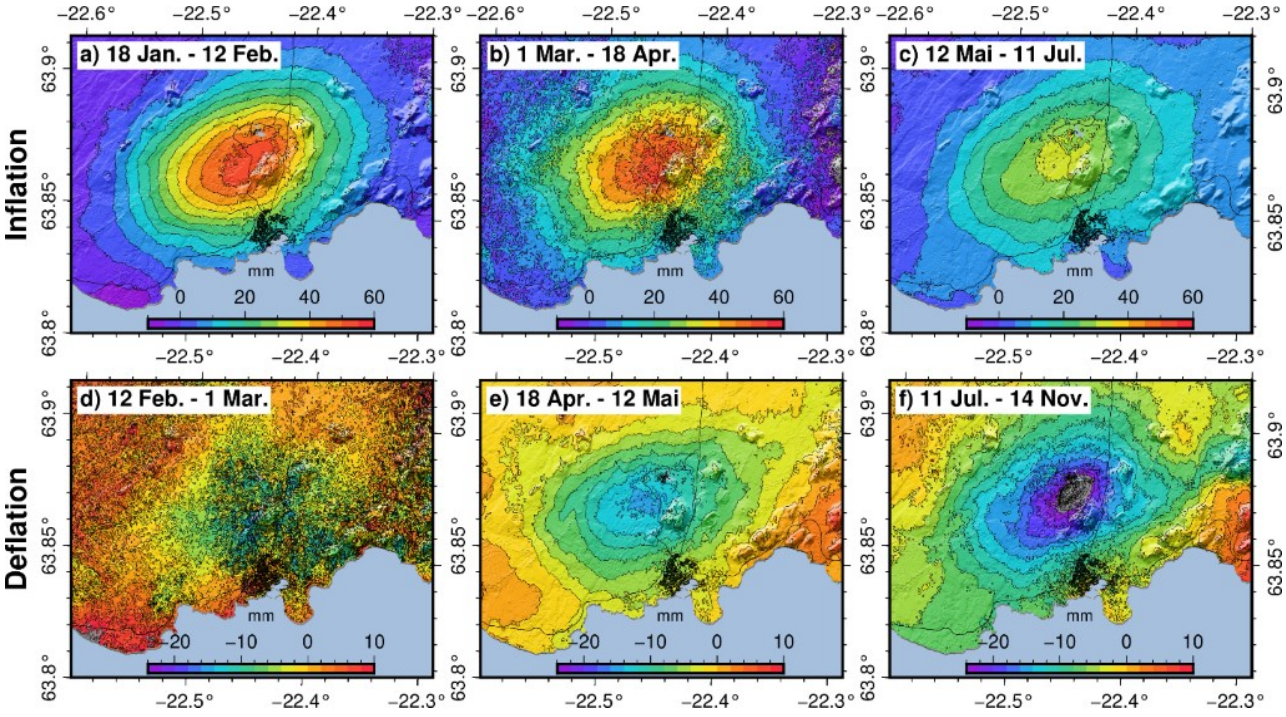

Figure 4: Near-Up displacement for the three inflation episodes and their subsequent deflation episodes. Background shows shaded topography, buildings (black areas), roads (black lines), and ocean (grey/blue areas).

6. SEISMICITY

The seismicity of the Reykjanes Peninsula with a focus on Svartsengi has been monitored by the network of the IMO (www.vedur.is) and HS Orka since 1997 (Ágústsson et al., 1998). Today, it is a part of the regional seismic network of Iceland, the SIL network, which is operated by the IMO. The coverage of the network remained the same from 1997-2008, when a seismic station was added at the tip of Reykjanes Peninsula in 2008. The network remained the same from 2008 to February 2020 when 5 stations were temporary added to the SIL system due to the 2020 seismic swarms. In this paper we use the IMO seismic catalogue for the period from 1995 to 2020. Denser temporary networks have been operated by research institutions and projects. Examples are the network of Klein et al. (1973 and 1977), the Hydrorift networks (Geoffrey and Dorbath, 2008, Kristjánsdóttir, 2013), the

IMAGE network by ÍSOR, GFZ and HS Orka, the Reykjanes network operated by ÍSOR for HS Orka, the DEEPEGS network by ÍSOR, KIT and HS Orka and the REYKJANET network operated by the Czech Academy of Sciences in cooperation with ÍSOR.

IMO runs an open interactive web service where the user can access the earthquakes in the IMO database that have been located by the SIL network (https://skjalftalisa.vedur.is). The web site allows the users to prepare maps and various predetermined plots and to apply various filters to select time, space, and size windows from the database and plot it interactively. Presently, the accessible database contains earthquakes form 2009 to present.

Figure 5 shows an example of the use of the database for the Reykjanes peninsula. It shows the spatial development of the earthquake activity year by year since 2009 to November 2020. From 2009 there is a typical background seismicity of the peninsula with almost persistent activity in the Krýsuvík high temperature area and three considerable seismic swarms are observed in the Fagradalsfjall area, i.e., in 2009, 2017 and by the end of 2019. The last one seems to mark the beginning of the intensive seismicity of 2020 that did spread out over almost all the seismic plate boundary of the Reykjanes Peninsula. Hence, the 2020 uplift and seismicity of the Svartsengi geothermal field is not only a local event, but a part of general movement of the oblique plate boundary along the peninsula. The seismicity of 2009 in Krýsuvík and Fagradalsfjall was analysed by Kristjánsdóttir (2013) and Guðnason (2014). The latter also observed induced seismicity in 2009 close to the re-injection wells of geothermal fluid in Svartsengi almost down to 5 km depth by using a dense temporary seismic network operated by the Science Institute of the University of Iceland in addition to the regional network. Since 2009 and until 2019, relatively few earthquakes are observed that are likely to be attributed to the re-injection.

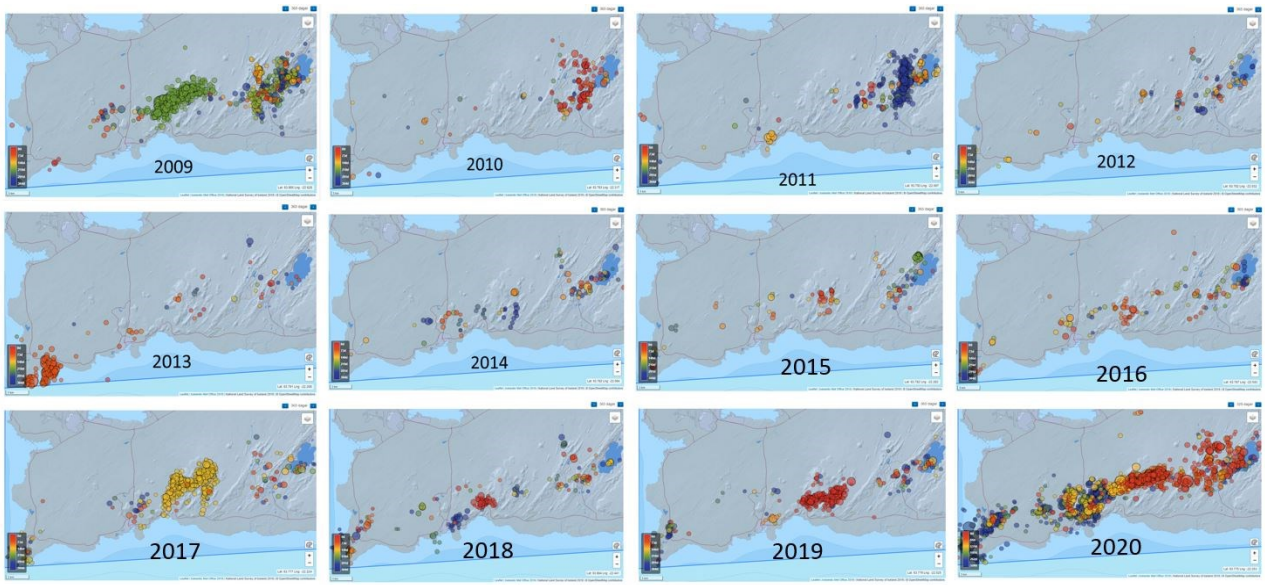

Figure 5: Annual earthquakes of magnitude 1.5 M_L and greater from 1.1.2009 to 24.11.2020 on the Reykjanes Peninsula. The different colours refer to the time of the year, red being the most recent ones and blue the oldest earthquakes. The plots are created by the IMO interactive web services (https://skjalftalisa.vedur.is).

Figure 6 shows the time evolution of seismicity of the entire Reykjanes Peninsula from Krýsuvík in the east to Reykjanes in the west during the 26 years period from 1995 to 2020. The magnitude of completeness is slightly less than magnitude 1 M_L (Figure 6) and the number of events in December 2019 to December 2020 above magnitude 1 M_L is about 2600. This is about 1/5 of the total number of events with magnitude above 1 M_L in the catalogue, or 20% occurring within less than 4% of the time of this 26-year period and is due to both the intense 2020 activity and a denser seismic network. Figure 5 highlights the swarm like behaviour of the seismicity in the peninsula. Especially noteworthy swarms are the swarm in 2003 is in the Krýsuvík area, the swarms in 2009 were simultaneously in Fagradalsfjall and Krýsuvík, the 2011 Krýsuvík swarm and the 2013 swarm east of the tip of Reykjanes and 2017 in Fagradalsfjall. The activity from December 2019 to December 2020 is characterised by intense seismic swarms with short intervals. It should be noted that the Svartsengi area has experienced fairly low seismicity rates over the last 11 years (Figure 5) compared to areas to the east and west.

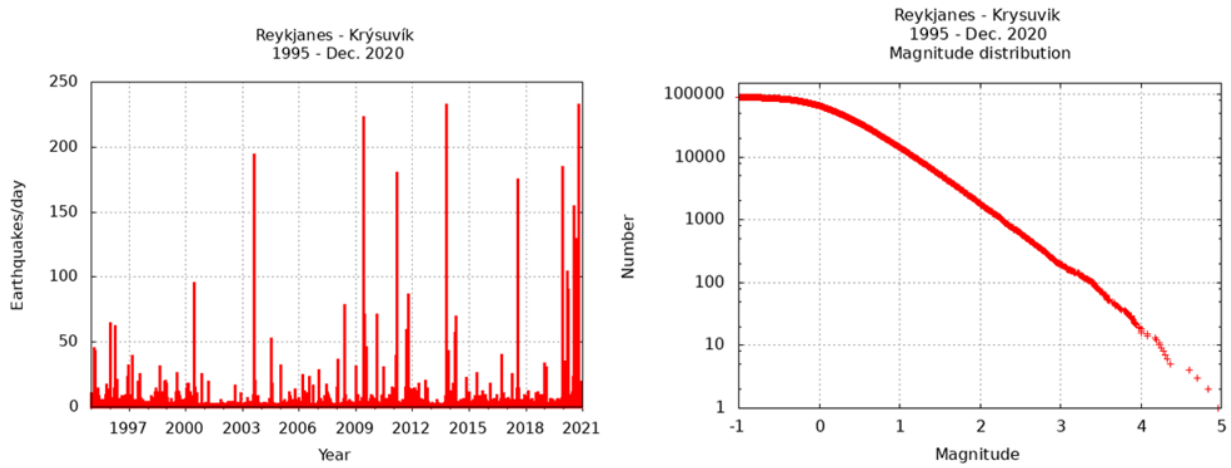

Figure 6: Overview of the seismicity on the Reykjanes Peninsula between Krýsuvík and Reykjanes from 1995. Left: Number of earthquakes per day Right: M_L magnitude distribution. The b-value is approximately 1.

6.1 Time evolution of the seismicity around Svartsengi

Figure 7 shows the time evolution of the seismicity and its depth distribution in and around the inflation area in Svartsengi from the onset of the seismicity in December 2019 to the beginning of December 2020 based on the IMO catalogue. The selected area is marked in Fig. 2 and covers the geothermal field. The figure clearly shows the swarm-like pattern of the seismicity separated by relatively quiet intervals.

It should be noted that the events in the IMO catalogue commonly show 1-2 km deeper hypocentres than the local denser networks with stations above or close to above the hypocentres. Then the depth is not as dependent on the velocity model as when the seismic stations are at greater distance. This effect has been demonstrated by Guðnason (2020) close to the Reykjanes power plant and appeared around Svartsengi after the improvement of the seismic network in February 2020. The apparent decrease in hypocentre depths in February in Fig. 7 is therefore an artefact and demonstrates the importance of a dense local network for reliable depth estimates. The hypocentral depths after February 2020 are therefore more reliable.

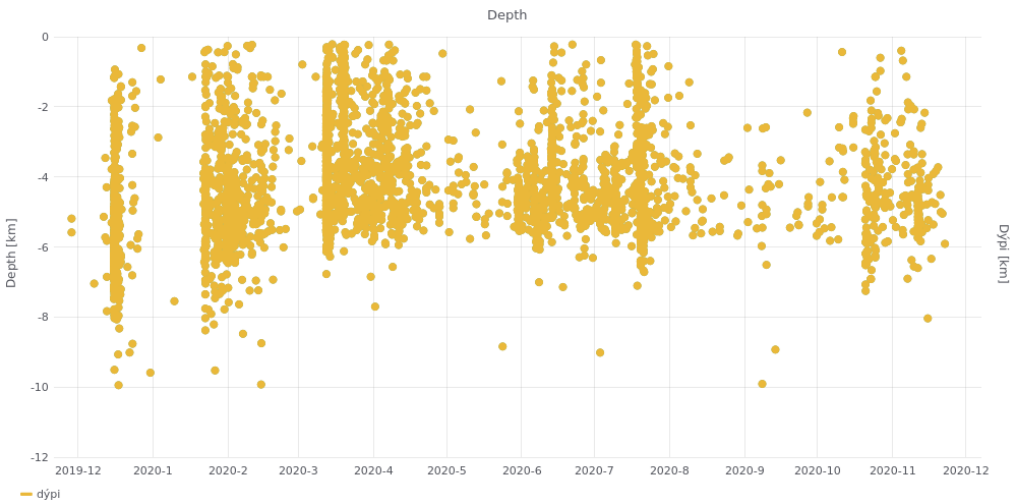

Figure 7: Seismicity in the research area (see Fig. 2 for definition) during the 2020 unrest episode plotted as depth vs. time. Note that the episode starts in December 2019. The apparent ~2 km decrease in the maximum depth of hypocentres in February 2020 is an artefact caused by insufficient coverage of local seismic stations until additional seismometers were installed in late February.

Figure 8 shows an overview of the seismicity and the near vertical deformation calculated from the InSAR data. When we compare the timing of the earthquakes to the deformation data, we must be careful due to the different time resolution of the two datasets. The seismic data has basic resolution of seconds, but Fig. 8 shows earthquakes per day. The InSAR data have much less resolution as they are based on satellite data that gives elevation changes with an interval of about a week. To compare the seismicity and the deformation in detail, continuous GPS measurements that give good elevation resolution using one day of data for each estimate must be used.

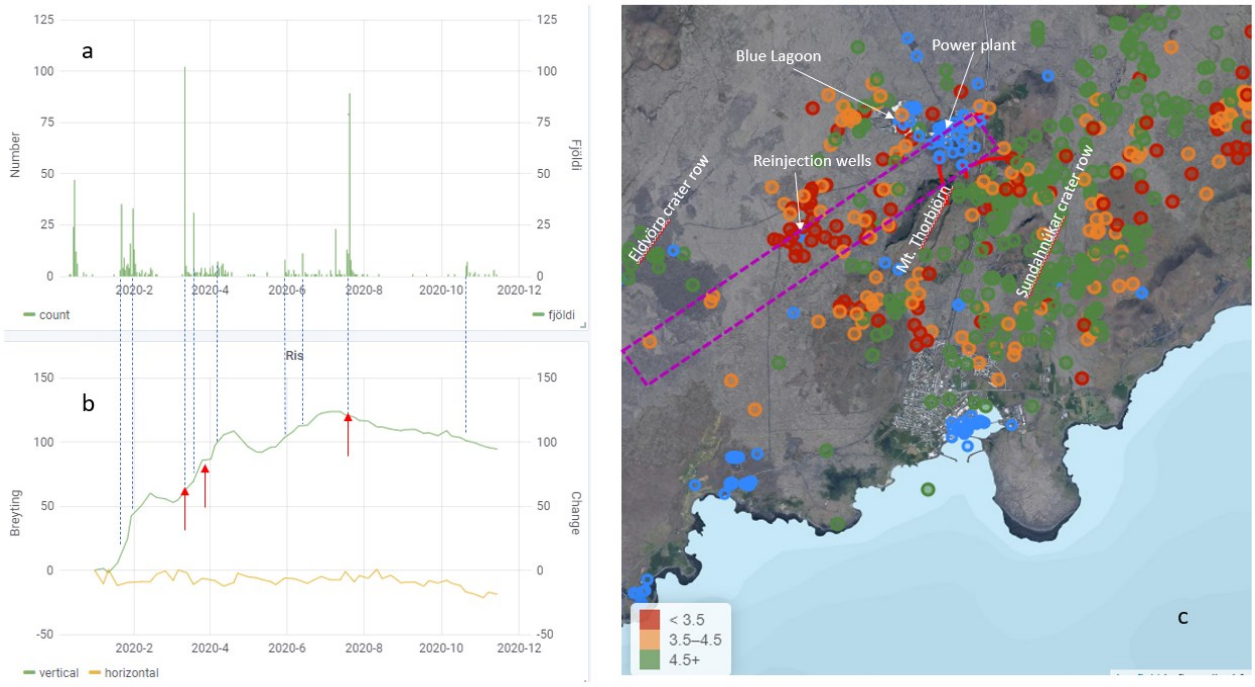

Figure 8: a) Number of earthquakes of M_L 1.0 and greater per day, b) Uplift in mm calculated from InSAR (near-Up) data from December 2019 to December 2020, c) Map view of earthquakes coloured by focal depth; red represents shallower events than 3.5 km; orange between 3.5 and 4.5 km depth and green deeper than 4.5 km depth. Blue circles are boreholes. The violet rectangular box shows the approximate location of the suggested intrusion as in Fig. 2.

Several interesting information can be derived from Figure 8 and a closer inspection of the individual swarms:

a) The first swarm of this sequence occurs in the middle of December 2019, W of Fagradalsfjall about 6 km SE of the centre of uplift. No uplift was detected in relation to this swarm.

b) The uplift and the second swarm started on January 21st, 2020. From the InSAR data it appears that the earthquake swarm started later than the uplift, but nearby GPS stations indicate that they started almost simultaneously. The location of the second swarm was around the Sundahnúkar crater row east of Mt. Thorbjörn and Sýlingafell, 2-4 km east of the centre of uplift. The depth distribution for this swarm is unreliable due to too sparse seismic network. Magnitudes up to M_L 3.3 were observed.

c) The third swarm occurred on January 31st during the continuous uplift phase, located within the Sundahnúkar crater row and just south of Mt. Thorbjörn. The earthquakes extend down to just over 6 km depth that might be an overestimate. Maximum magnitude was M_L 3.7.

d) The fourth swarm started on March 12th, mostly within the Sundahnúkar crater row and extending farther eastwards to Fagradalsfjall. The focal depth was down to around 6 km and maximum magnitude was M_L 4.2. This swarm did also extend westwards almost to the eastern boarder of the Svartsengi production field between Mt. Thorbjörn and Sýlingafell.

e) On March 19th, a swarm occurred above the centre op uplift, centred around the re-injection wells. Most of these earthquakes occurred above 3.5 km depth, only a few down to 4.5 km depth, maximum magnitude was M_L 2.9.

f) On May 30th and June 6th, small swarms occurred in the southernmost part of the Sundahnúkar crater row, close to the town of Grindavík. The depth extends down to 5.5 km and maximum magnitude was M_L 2.2.

g) On June 6th and 13th, a small swarm with shallow earthquakes occurred close to the centre of uplift and also down to 5.0 km beneath the Blue Lagoon with maximum magnitude of M_L 2.7.

h) On July 9th, a swarm occurred about 1 km east of the southern part of Sundahnúkar crater row, extending down to 5.7 km with maximum magnitude of M_L 2.8.

i) On July 18th, an intensive swarm happened above the proposed intrusion in-between the production field and the re-injection field. Most of the earthquakes are above 4.5 km depth but 3 are somewhat deeper. This swarm contained two earthquakes of M_L size 3.2 and 3.4 at 2.3 and 2.5 km depth.

j) On July 20th, a swarm occurred in the western part of Fagradalsfjall, 5-6 km east of the centre of uplift. Maximum magnitude was M_L 3.1.

k) On October 20th, a swarm of maximum magnitude M_L 2.0 was observed in the western part of Fagradalsfjall. In the following week it extended westwards as small, scattered earthquakes to the southern part of the Sundahnúkar crater row and the area south of Mt. Thorbjörn and to the town of Grindavík.

l) On November 11th, a localized swarm occurred in the northern part of the Sundahnúkur crater row. Maximum depth of hypocentres was close to 5.8 km and the largest magnitude was M_L 2.1.

The above description of the seismicity describes just the main trend. It is obvious that some of the swarms are composed of several closely spaced subswarms on different fissures. Detailed analysis is necessary to unravel the actual tectonic pattern and processes during the rifting of the plate boundary and the related uplift. This can be a topic for several PhD studies.

On Figure 8 we observe that the swarms occur always during the uplift period while there is very little seismicity during the deflation periods. Furthermore, the first swarm after each deflation period first occur when the uplift has exceeded its previous elevation. This is like the well-known Kaiser effect that is commonly observed during repeated fluid injection during stimulation of geothermal wells. It has for example been observed during re-injection into the Hellisheiði geothermal field where in the full-scale re-injection of 550 L/s that started in September 2011, no earthquakes occurred until the re-injection rate reached the 250 L/s that was the rate during drilling and excitation of one of the re-injection wells (Ágústsson et al., 2015). Similar Kaiser effect on larger scale has been reported in Icelandic volcanoes (e.g., Heimisson et al., 2015).

If we look carefully at the seismicity above the core of the geothermal field where the proposed intrusion is (Figure 8), we see high seismicity during the inflation phase and low seismicity in-between the two first uplift periods. This behaviour is expected due to the bending of the "roof" over the source of uplift. During the first uplift period, the seismicity is scattered over the entire core of geothermal field as defined in Fig. 2. During the second and the third uplift periods, the seismicity is more concentrated in the area from the re-injection field and towards and around the production field. It is noteworthy that no seismicity is observed within or below the production field itself which can be explained by the large pressure drawdown that increases the overall strength of the rock by lowering the pore pressure.

The last large swarm above the geothermal field occurred on July 18th, a few days after a slow deflation started. It was followed by the intensive swarm in Fagradalsfjall on July 20th. Since then, the seismicity within and in the vicinity of the geothermal field has decayed with time in correlation with continued deflation. In middle of November, the uplift was almost at the same level as before the third inflation phase.

6.2 Source mechanisms of the main earthquakes

Moment tensor solutions were calculated for the 46 events of $M_L > 2.5$ that occurred in the vicinity of Mt. Thorbjörn from January until April 2020. The earthquake source mechanisms are calculated using the MTFIT software (Pugh and White, 2018). These are full DC moment tensor inversions for the P-wave polarity phases, using the take-off angles in the calculations (of both P- and S-arrivals). All earthquakes were detected and located using both the P- and S-wave arrival in SeisComP (https://www.seiscomp.de/), then manually refined and relocated using the NonLinLoc (Lomax et al., 2000) software. The velocity model used is a gradient version of the standard SIL model with a constant Vp/Vs ratio of 1.78. The SIL velocity model is based on an analysis of a part of a refraction profile in the South Iceland Lowland (Bjarnason et al., 1993). This part of the refraction profile is from an area with dense, eroded rock which is expected to have a higher velocity in the shallower layers than the younger, less eroded rock in the area around Mt. Thorbjörn. The model is therefore not ideal for the Reykjanes Peninsula, but however, used for routine analysis at IMO and ÍSOR on the Reykjanes Peninsula.

The analysed events are fairly well constrained and are all stable, due to a good distribution of stations over the focal sphere, with the closest stations at less than 2 km from the centre of uplift since the end of February. These preliminary analyses show that the moment tensor solutions are mainly strike-slip, some normal faulting (and oblique normal faulting) is also observed. Strike-slip motion is observed across the area, but normal faulting is confined to the near east of Mt. Thorbjörn. A prominent trend is observed between the general orientation of the surface fissures and fractures (Figure 9a) and the P-axis (red dots on bottom Figure 9b). A few thrust faults are observed, an oblique one is located at the centre of the uplift on March 19th, 2020 (Figure 9a). To get a more in-depth understanding of the earthquake source mechanisms and the stress state of the crust in this area, more events over a wider magnitude and time range need to be analysed with a more appropriate velocity model.

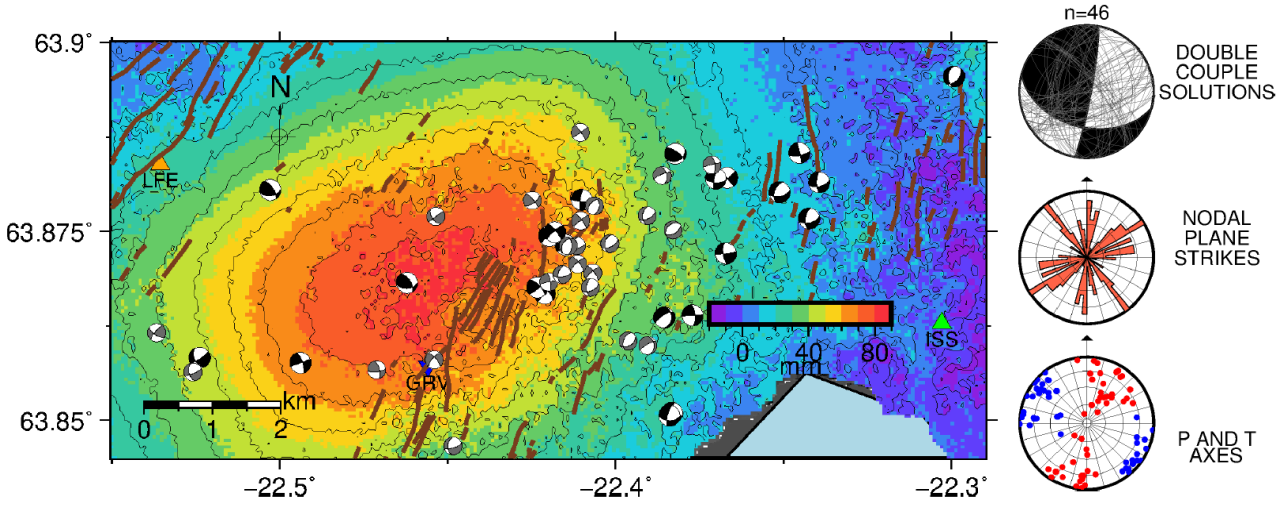

Figure 9: Left: The map displays the earthquake source mechanisms plotted on top of the near-Up displacement interferogram from January to April; the centre of uplift is to the west of Mt. Thorbjörn. Gray, smaller beach balls are less well constrained solutions from January-February 2020, black are better constrained solutions from March 1st to April 1st, 2020, after 5 additional seismic stations were put online. Blue inverted triangle is the IMO station GRV, green triangle is the CAS station ISS, and the orange triangle is the IMO/ÍSOR station LFE. Brown faults and fractures are from Sæmundsson et al. 2016. Right: A rose diagram showing the nodal planes, strikes of both planes and the P (red) and T (blue) axes, respectively.

7. OTHER OBSERVATIONS

Time-lapse gravity measurements at permanent sites may reveal density variations with time which in case of the uplift west of Mt. Thorbjörn could be caused by magma intruding into the subsurface and/or other density changes in the underground. As soon as the uplift was realized, it was decided to measure gravity at fixed locations. The objective was to have a baseline of gravity as a reference to monitor density variations if the uplift would continue.

Gravity was measured in the uplift area around Mt. Thorbjörn at 10-12 permanent sites in three successive campaigns. The first campaign was a couple of days after the realization of the uplift on January 28th and 29th. At that time, the total uplift was already almost 4 cm. The second campaign was between April 22nd and 28th when the total uplift was a bit more than 10 cm, or around 6.5 cm since the first campaign. The last gravity campaign was conducted on October 5th and 6th, when the total net uplift was a bit more than 11 cm or about 1 cm since the last campaign.

Figure 10 shows the gravity changes between the first and second, and the second and third campaigns. The gravity values have been corrected for the elevation changes between the two campaigns (free-air corrected) using InSAR data. Elevation and gravity at the second northernmost side (point HS22) was used as reference point but corrected for uplift at this site of 5 mm during the period between the first and third campaign. The uncertainty in a campaign like this one is on the order of 10-15 µgal. The gravity value at the end points (HS16 and SNH25) are less constrained and regarded unreliable.

Gravity changes between the first and second campaign indicate consistent 10-16 µgal gravity increase close to the production field and the centre of inflation. On the contrary, there seems to be a consistent gravity decrease of up to 8 µgal from April to October around the centre of uplift. Altogether these sites show a small gravity increase of up to 10 µgal between the first and third campaign which is within the level of significance. The ground water level in a water well just west of Grindavík was 70-80 cm higher in October than in the beginning of March. If similar increase in groundwater level occurred in the area around Svartsengi, it would lead to 6 µgal gravity increase if the average porosity is 20%. This can, therefore, contribute to the overall gravity increase from February to October. It can be concluded from the gravity measurements that a possible free air gravity increase in connection with the inflation is not higher than 10-12 µgal during the first months and there are indications of slight gravity increase after that.

Michelle Parks at IMO has kindly provided us the coordinates of the proposed horizontal intrusions that can explain the uplift of the surface. For simplicity, we have merged them into a single plank-like body at 3.8 km depth. The length of the body is assumed to be 5.5 km, the width is 0.4 km, and its thickness is 2.8 m (Figure 2) which equals to 6.300.000 m^3 of volume increase. By assuming the density of this plank to be 2,700 kg/m^3, we calculate the maximum value of the gravity increase above the centre of the plank to be 11 µgal. With respect to possible changes in the ground water level, the uncertainty of the gravity measurements and the shape of the measured changes in gravity, it cannot be stated that the signal measured reflects significant gravity increase from the source of the uplift.

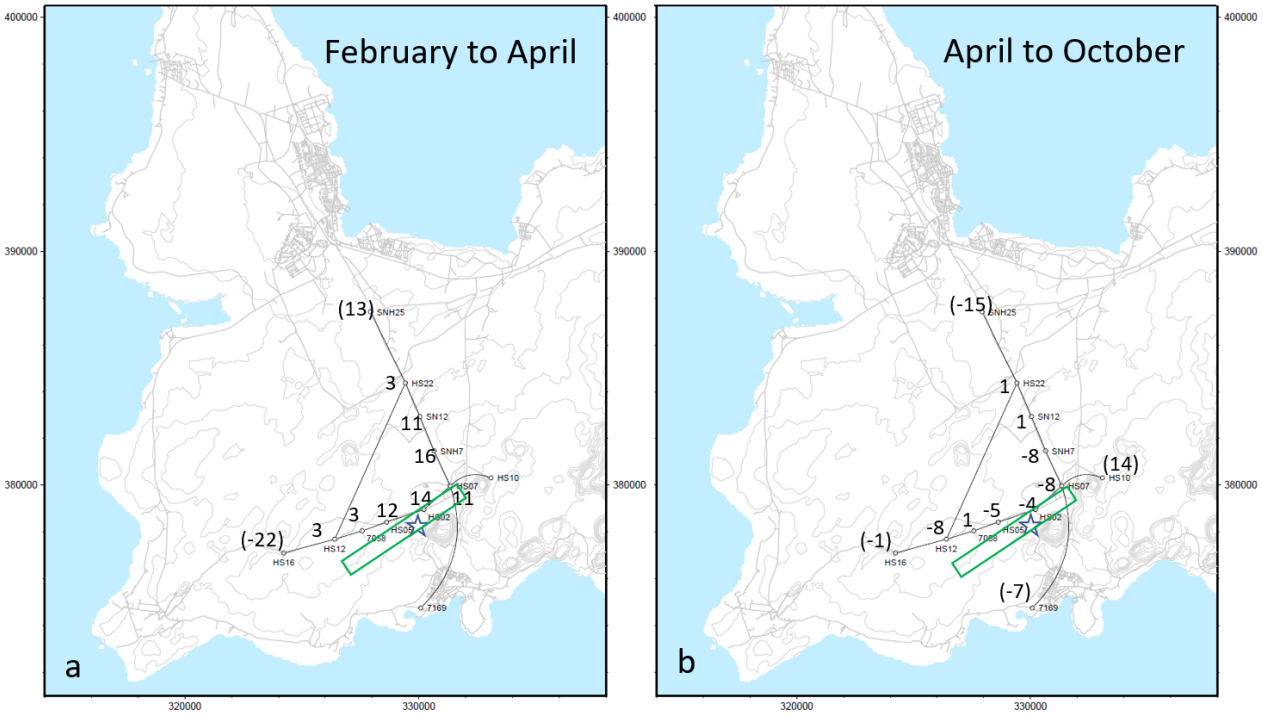

Figure 10: Observed free-air corrected gravity changes in µgal. a) Gravity changes from January 28th - 29th to April 22nd - 28th. b) Gravity changes from April 22nd - 28th to October 5th-6th. The green rectangular shows approximate location of the proposed sill and the blue star the centre of uplift.

Extensive resistivity surveys have been performed around the Svartsengi geothermal field, applying both the TEM and MT method to delineate and investigate the geothermal resource. The data have been 3D inverted resulting in a resistivity model of the area (Karlsdóttir et al., 2020). It is not an easy task to measure resistivity close to a power plant and the associated pipes and high voltage power lines. However, three of the measurement sites close to the main uplift and showing a fairly good data quality were re-measured during the summer of 2020. The objective was to investigate if resistivity changes since the beginning of the uplift could be inferred. A simple 1-D modelling indicates that resistivity changes due to thin conductive sill at 4km depth like the proposed source of the uplift (Fig. 2a) will be difficult if not be impossible to detect.

HS Orka has monitored the gas content of the steam in production wells in order to detect possible change within the geothermal reservoir. Until December 2020, no such changes have been observed (Guðjón Helgi Eggertsson, pers.com.).

8. DISCUSSION

Understanding of the processes that have been ongoing beneath and close to the Svartsengi high temperature field is extremely important from the perspective of civil protection including the security of people, the village of Grindavík and the Svartsengi Resource Park. Severe disturbances, and in the worst-case, complete shut-down of the energy production in Svartsengi or its transmission pipelines will turn off heat and water supply for the entire area, including the Keflavik international airport and will have severe economic consequences. Therefore, the unrest in Svartsengi and on the Reykjanes Peninsula has been subject to lively discussions in the Icelandic geoscientific community where various scientists and groups have collected data and interpreted as soon as possible. Ideas and interpretation of data sets have been presented at local conferences during the unrest period, but formal scientific publications are not yet available.

It is evident that the seismicity in 2020 is a regional tectonic event that shows rifting and movement of the plate boundary along almost the entire Reykjanes Peninsula. In the view of the past seismic behaviour of the plate boundary, a major rifting episode was about due in time.

The development of the unrest raises several key questions on cause and effects. Did the earthquakes that started in the Sundahnúkar area on January 22nd 2020 lead to a process that caused immediate uplift below the Svartsengi geothermal field or is the initiation of the seismicity caused by sudden pressure and volume increase in the roots of the Svartsengi geothermal field? Due to low time resolution of the uplift data, it is difficult to conclude what came first on January 22nd, the earthquakes or a pressure pulse from the first phase of the uplift. However, it seems clear, that the start of the second and the third uplift episodes was followed by large earthquake swarms. This indicates that the earthquakes were triggered by pressure pulses from the source of uplift. It seems therefore reasonable to assume the same for the start of the first episode. By inspecting Figure 5 carefully, repeated small seismic swarms and scattered earthquakes occur in the Sundahnúkar area during most of the years from 2009 to 2019, especially in 2017 and 2018. This indicates that the fault systems close to Sundahnúkar was critically stressed, and only a minor pressure disturbance could lead to the onset of a large-scale movement of the plate boundary. Therefore, it is reasonable to assume

that pressure and volume increase at approximately 4 km depth beneath the centre of the Svartsengi geothermal field triggered the seismicity of 2020.

This leads to the important question of the nature and the cause of the volume and pressure increase. In any case, material is needed that can intrude into the crust or expand to create pressure that is enough to lead to uplift of the overlying crust. One prerequisite to evaluate different possibilities is to estimate possible conditions at the source of uplift at 4-4.5 km depth. The B/D boundary beneath Svartsengi seems to be at around 5 km depth, about 1 km shallower than for the surrounding area. In analogy with the results from the IDDP-2 well at Reykjanes high temperature field (Friðleifsson et al., 2020) we can expect temperatures of 500-700°C close to 5 km depth, some permeability and under-pressure with respect to a cold-water column. It is also likely that the top of the lower crust is close to 4.5 km, so the source of uplift is most likely closely above the top of the lower crust where we expect the rocks to be made of 100% dykes. In addition, cooling magmatic intrusions into the upper crust are generally supposed to be the heat source of high temperature fields. It is therefore reasonable to suspect a magmatic intrusion to cause of uplift in Svartsengi.

However, there are several observations that discredit or do not support the idea of magmatic intrusion as the only cause of the uplift. Firstly, there have not been observed any seismic indications of dyke formation or paths where magma is being transported from the mantle or deep crustal layers to the source of uplift. Such evidence is known to accompany magmatic movements and dyke formation like happened in the Krafla fires in 1976-1984 (e.g. Wright et al., 2012), in the formation of Holuhraun in 2014 (e.g. Sigmundsson et al., 2015, Ágústsdóttir et al., 2016) and during the unrest beneath Upptyppingar in 2007 (e.g. Vilhjálmsson and Flóvenz, 2017, White et al., 2011, White et al., 2019). This is however not a necessary condition for dyke formation or magma transport since the movement might have been completely within the ductile part of the crust. Secondly, no increase in gas concentration or gas composition in the geothermal fluid has been reported but possibly it will take the magmatic gasses long time to diffuse from 4 km depth into the main production field at 1-2 km depth. Thirdly, the deflation after the uplift period is very difficult to explain if the uplift was only caused by intrusion of magma. Some volume reduction could be expected to follow solidification of a magma body but hardly more than 10% (Petersen, 1987, Wittman et al., 2014). In case of the Svartsengi, the cumulative uplift of the three episodes equals almost 150 mm while the subsidence equals almost 60 mm or around 40% for 11 months. Correcting for the estimated long-term subsidence of 12 mm/year caused by the geothermal production results in around 30% volume reduction.

One possibility to explain the large deflation is interaction between intruded magma and fluid within the roots of the geothermal system. In this case, the intruded magma comes into contact with or transfer heat indirectly into an aquifer where the fluid is present in liquid state which then boils, expands to high enough pressure to lift the overburden. Then the fluid diffuses along a permeable aquifer or porous rock and causes much larger deflation than compaction due to solidification can account for. Similar effects are expected if the intruded material contains considerable amount of gas like CO_2.

Still another possibility is that the pressure source is a pure fluid phenomenon where relatively cold water intrudes 600-700°C hot rock at 4-5 km depth, boils and expands and then diffuses slowly away causing deflation. The experience from well IDDP-2 at Reykjanes shows downflow of cold injected fluid into an aquifer at 4.5 km depth where the temperature is close to 600°C. This implies that there is permeability at these P-T conditions, or alternatively that the pressure from the cold-water column in the well is high enough to create permeability at that depth. This shows furthermore that the strength of the rock just above the B/D boundary is high enough to maintain open fractures and the pore pressure is not yet lithostatic as is expected below the B/D boundary. The generally accepted conceptual model of the high temperature fields assumes that cold groundwater sinks somewhere into the deep hot rocks of the geothermal system, preferably along permeable fault zones, where it is heated and flows toward the surface. Although there is no shortage of cold water in the highly permeable near surface rocks close to Svartsengi, the natural recharge might be hampered by the clay cap that isolates the geothermal system from the groundwater above. The re-injection wells solve this problem as the ~95°C hot re-injection liquid exits the wells into near vertical fracture at close to 1 km depth where the rock temperature exceeds 200°C. There, the re-injection fluid sinks along the fractures and heats slowly up and consequently cools the walls of the fault that contracts and widens downward with time. How far into the ground the fracture will extend is not known, but it might take many years to reach the 4-5 km depth of the B/D boundary. However, there is no direct evidence that such expanding fluid is derived from re-injection, but the location of the centre of uplift close to the re-injection wells, as well as the concentration of seismicity in 2020 around the re-injection wells gives indications.

Above, we have discussed three possible explanations of the cause of the vertical displacement in Svartsengi high temperature field and the related seismicity. In addition, intrusion of mantle-derived carbon dioxide might be a possibility to explain the inflation-deflation patterns. This possibility is supported by abnormal low Vp/Vs ratio, especially at 4-6 km depth, that has been reported very close to Svartsengi and suggested to be due to supercritical fluids (Geoffroy and Dorbath, 2008). Similar explanation was proposed for observed low Vp/Vs ratio beneath the Hengill high temperature and volcanic system (Tryggvason et al, 2002).

We conclude from our preliminary analysis of the available data that there are several possibilities to explain the pressure increase that caused the uplift and probably triggered the nearby seismicity. To examine these different possibilities, it is necessary in future modelling to account for the high temperature, pressure, and permeability at the source of uplift and possible interaction between magma intrusion, gas content and the in-situ geothermal fluid. Our present evaluation of the available data does not prove or disprove any of the hypotheses on the origin of the pressure and volume increase at the source of uplift.

ACKOWLEDGEMENT

The authors are grateful to the geoscience society in Iceland, the colleagues at ÍSOR, GFZ in Potsdam, the Cech Academy of Sciences, IMO, IES and HS Orka as well as others that have contributed to data acquisition and the fruitful and open discussions about the interesting unrest period at the Svartsengi high temperature field and the rifting of the plate boundary of the Reykjanes Peninsula. These events will lead to number of scientific publications that will contribute to the understanding of the processes involved. In this context, openness and sharing of data is of vital information for the scientific process. Special thanks to Michelle

Parks of IMO who provided the source parameters for the intrusion model, Albert Þorbergsson of ÍSOR for assisting with maps and the excellent work of IMO in operating and maintaining the national seismic network and the open access to the seismic catalogue.

REFERENCES

Albertsson, A, and Jónsson, J.: The Svartsengi Resource Park, *Proceedings of the World Geothermal Congress*, Bali, Indonesia, (2010), 2p.

Ágústsdóttir, T., Woods, J., Greenfield, T., Green, R.G., White, R.S., Winder, T., Brandsdóttir, B., Steinthórsson, S. and Soosalu, H.: Strike-slip faulting during the 2014 Bárðarbunga-Holuhraun dike intrusion, central Iceland. *Geophysical Research Letters*, **43(4)**, (2016).1495-1503.

Ágústsson, K., Rögnvaldsson. S. Th., Bergsson. B. H. and Stefánsson, R..: Jarðskjálftamælanet Veðurstofu Íslands og Hitaveitu Suðurnesja. *VÍ-R98002-JA02,* Reykjavík, Febrúar 1998 (In Icelandic).

Ágústsson, K. and Flóvenz, Ó.G.: The Thickness of the Seismogenic Crust in Iceland and its Implications for Geothermal Systems. *Proceedings of the World Geothermal Congress*. Antalya, Turkey. (2005), 9p.

Ágústsson, K., Kristjánsdóttir, S., Flóvenz, Ó. G. and Guðmundsson. Ó.: Induced Seismic Activity during Drilling of Injection Wells at the Hellisheiði Power Plant, SW Iceland. *Proceedings World Geothermal Congress*, Melbourne, Australia, 19—25 April 2015.

Axelsson, G., Arnaldsson, A., , Berthet, J.C., Bromley, C.J., Gudnason, E.Á., Hreinsdóttir, S., Karlsdóttir, R., Magnússon, I.Th., Michalczewska, K.L., Sigmundsson, F., and Sigurdsson, Ó.: Renewability Assessment of the Reykjanes Geothermal System, SW-Iceland, *Proceedings of the World Geothermal Congress*. Melbourne, Australia. (2015), 10p

Bali, E., László, E.A., Zierenberg, R., Diamond.L.W, Pettke, T., Szabó, Á., Guðfinnsson, G.H., Friðleifsson. G.Ó. and Szabó,C.: Geothermal energy and ore-forming potential of 600 °C mid-ocean-ridge hydrothermal fluids: *Geology*, **48** (2020) 5p, https://doi.org/10.1130/G47791.1

Berardino, P., Fornaro, G., Lanari, R., and Sansosti, E.: A new algorithm for surface deformation monitoring based on small baseline differential SAR interferograms, *IEEE Transactions on Geoscience and Remote Sensing*, vol. **40**, no. 11, pp. 2375-2383, (2002), doi: 10.1109/TGRS.2002.803792.

Bjarnason, I.Th., Menke, W., Flóvenz, Ó.G. and Caress, D.: Tomographic image of the Mid-Atlantic Plate Boundary in southwestern Iceland. *JGR, volume **98**, issue B4,* (1993).

Björnsson, S., Einarsson, P., Tulinius, H., and Hjartardóttir, Á., R.: Seismicity of the Reykjanes Peninsula 1971-1976, *Journal of Volcanology and Geothermal Research*., **391** (2020), 19p.

Blanck, H., Jousset P., Hersir, G.P., Ágústsson, K., and, Flóvenz, Ó.G.: Analysis of 2014–2015 on- and off-shore passive seismic data on the Reykjanes Peninsula, SW Iceland, *Journal of Volcanology and Geothermal Research*., **391** (2020), 10p.

De Freitas, M., Numerical modelling of subsidence in geothermal reservoirs: Case study of the Svartsengi geothermal system, SW-Iceland. *United Nations University Geothermal Training Programme* Reykjavík, Iceland. (2018) 62p.

Darbyshire Fiona A., White, Robert S., Priestley, Keith F.: Structure of the crust and uppermost mantle of Iceland from a combined seismic and gravity study, *Earth and Planetary Science Letters* 181 (2000) **409**-428.

Einarsson, P.: Plate boundaries, rifts and transforms in Iceland, *Jökull*, **58**, (2008), 35-58.

Eysteinsson, H.: Elevation and gravity changes at geothermal fields on the Reykjanes peninsula, SW-Iceland, *Proceedings, World Geothermal Congress,* Kyushu-Tohoku, Japan, (2000), 559–564

Flóvenz, Ó.G.: Seismic structure of the Icelandic crust above Layer Three and the relation between body wave velocity and the alteration of the basaltic crust, *J. Geophys.,* **47,** (1980) 211–220.

Franzson, H.: The Svartsengi high-tenperature field, Iceland. Subsurface geology and alteration, Geothermal Resources Council, *Transactions* **Vol. 7**, (1983), 141-145.

Franzson, H.: Svartsengi, Jarðfræðilíkan af háhitakerfi og umhverfi þess. *Orkustofnun*, **OS-90050/JHD-08**, (1990), 41p.

Friðleifsson, G.Ó., Elders, W.A., Zierenberg, R.A., Fowler, A.P.G., Weisenberger, T.B., Mesfin, K.G., Sigurðsson, Ó., Níelsson, S., Einarsson, G., Óskarsson, F., Guðnason, E.Á., Tulinius, H., Hokstad, K., Benoit, G., Nono, F., Loggia, D., Parat, F., Cichy, S.B., Escobedo, D. and Mainprice, D.: The Iceland Deep Drilling Project at Reykjanes: Drilling into the root zone of a black smoker analog. *Journal of Volcanology and Geothermal Research* **391** (2020) 106435.

Friðleifsson, G.,Ó., Sæmundsson, K., and Þórhallsson, S.: Lághitaleit á Rosmhvalanesi 2000-2001, Hitastigulsholur RH-03, RH-04 og RH-05. *Orkustofnun*, **OS-2002/055**, (2002) 39p.

Geoffroy, L., and Dorbath, C.: Deep downward fluid percolation driven by localized crust dilatation in Iceland, *Geophysical Research Letters,* **35**, l17302, doi:10.1029/2008GL034514, (2008), 6p.

Guðnason, E., Á.: Analysis of seismic activity on the western part of the Reykjanes Peninsula, SW Iceland, December 2008 – May 2009, Master's thesis, Faculty of Earth Sciences, University of Iceland, (2014), 83p.

Guðnason, E., Á.: Presentation at ISOR annual meeting, (2020), https://www.youtube.com/watch?v=rivngjnRg3Y.

Heimisson, E.R., Einarsson,P., Sigmundsson,F. and Brandsdóttir, B.: Kilometer-scale Kaiser effect identified in Krafla volcano, Iceland, *Geophys. Res. Lett*., **42**, 7958–7965,doi:10.1002/2015GL065680, (2015)

Hersir, G.P., Árnason,K., Vilhjálmsson, A.M., Saemundsson K., Ágústsdóttir, Þ., and Friðleifsson, G.Ó.: Krýsuvík high temperature geothermal area in SW Iceland: Geological setting and 3D inversion of magnetotelluric (MT) resistivity data. *Journal of Volcanology and Geothermal Research* **391** (2020) 106500.

Hjartarson, Á, and Sæmundsson, K.: Geological map of Iceland, bedrock, 1:600,000, Iceland GeoSurvey, Reykjavík (2014)

Kaban, M.K., Flóvenz, Ó.G., and Pálmason, G.: Nature of the crust-mantle transition zone and the thermal state of the upper mantle beneath Iceland from gravity modelling. *Geophys. J. Int*. (2002) **149**, 281–299.

Karlsdóttir, R.: TEM-viðnámsmælingar í Svartsengi. *Orkustofnun*, **OS-98025**, (1998), 43p.

Karlsdóttir, R., Vilhjálmsson, A.M., and Guðnason, E.Á.: Three dimensional inversion of magnetotelluric (MT) resistivity data from Reykjanes high temperature field in SW Iceland, *Journal of Volcanology and Geothermal Research*, **391** (2020), 14p.

Klein, F. W., Einarsson,P., andWyss, M.: Microearthquakes on the Mid-Atlantic plate boundary on the Reykjanes Peninsula in Iceland. *J. Geophys. Res*., **78** (1973) 5084—5099.

Klein, F. W., Einarsson,P., andWyss, M.: The Reykjanes Peninsula, Iceland, earthquake swarm of September 1972 and its tectonic significance, *J. Geophys. Res*., **82**, (1977), 865– 888.

Kristjánsdóttir, S.: Microseismicity in the Krýsuvík Geothermal Field, SW Iceland, from May to October 2009, *M.Sc. thesis, Faculty of Earth Sciences, University of Iceland*, (2013), 70p.

Lomax, A., Virieux, J., Volant, P. and Berge-Thierry, C.: Probabilistic Earthquake Location in 3D and Layered Models. In: Thurber C.H., Rabinowitz N. (eds.)*, Advances in Seismic Event Location. Modern Approaches in Geophysics*, *vol. **18***., (2000). Springer, Dordrecht.

Orkustofnun.: https://orkustofnun.is/gogn/Talnaefni/OS-2020-T009-01.pdf, (2020).

Pálmason, G.: Crustal structure of Iceland from explosion seismology, Soc. Sci. Isl., Reykjavik, **XL**, Iceland, (1971), 9–187.

Pálmason, G.: Jarðhitabók, eðli og nýting auðlindar. *Hið íslenska bókmenntafélag*, Reykjavík (2005), 298p.

Petersen J., S.: Solidification contraction: another approach to cumulus processes and the origin of igneous layering. In: Parsons I (ed) *Origins of igneous layering*. **D. Reidel, Dodrecht**, (1987), 505–526.

Pugh, D. J. and White, R. S.: MTfit: A Bayesian approach to seismic moment tensor inversion, *Seismological Research Letters*, ***89(4)**, (2018),* 1507-1513.

Sigmundsson, F., Hooper, A., Hreinsdóttir, S., Vogfjörd, K.S., Ófeigsson, B.G., Heimisson, E.R., Dumont, S., Parks, M., Spaans, K., Gudmundsson, G.B. and Drouin, V.:Segmented lateral dyke growth in a rifting event at Bárðarbunga volcanic system, Iceland. *Nature*, **517(7533)**, (2015),191-195.

Sæmundsson, K., Sigurgeirsson, M.Á., Hjartarson, Á., Kaldal, I., Kristnsson, S.G., and Víkingsson.; Geological map of Southwest Iceland, 1:100,000, 2nd ed., *Iceland GeoSurvey*, Reykjavík, (2016).

Sæmundsson, K., and Sigurgeirsson, M.Á.: Reykjanesskagi. In Sólnes et al (ed): Náttúruvá á Íslandi, *Viðlagatrygging Íslands/Háskólaútgáfan, (2013), 379—401.*

Sæmundsson, K., Sigurgeirsson, M.,Á., and Friðleifsson, G.Ó.: Geology and structure of the Reykjanes volcanic system, Iceland. *Journal of Volcanology and Geothermal Research*, **391** (2020), 12p. https://doi.org/10.1016/j.jvolgeores.2018.11.022

Tryggvason, A., Rögnvaldsson, S.Th., and Flóvenz, Ó.G.: Three-dimensional imaging of the P- and S-wave velocity structure and earthquake locations beneath Southwest Iceland. *Geophys. J. Int*. **151**, (2002) 848–866.

White, R.S., Edmonds, M., Maclennan, J., Greenfield, T. and Agustsdottir, T.: Melt movement through the Icelandic crust. *Philosophical Transactions of the Royal Society* **A, 377**(2139), 20180010 (2019).

White, R.S., Drew, J., Martens, H.R., Key, J., Soosalu, H. and Jakobsdóttir, S.S., 2011. Dynamics of dyke intrusion in the mid-crust of Iceland. *Earth and Planetary Science Letters*, **304(3-4**), (2011), 300-312.

Wittmann, W., Sigmundsson, F., Dumont, S.C.C. and Ófeigsson, B.G., Modelling of thermal contraction of emplaced lava flows at Hekla volcano. *Geophysical Research Abstracts*, **16**, EGU2014-11009, 2014 EGU General Assembly (2014).

Vilhjálmsson, A.M. and Flóvenz, Ó.G.: Geothermal Implications from a Resistivity Survey in the Volcanic Rift Zone of NE-Iceland and Comparison with Seismic Data." *Iceland GeoSurvey, Report,* **ÍSOR-20017/065**, (2017), 46p.

Wright, T.J., Sigmundsson, F., Pagli, C., Belachew, M., Hamling, I.J., Brandsdóttir, B., Keir, D., Pedersen, R., Ayele, A., Ebinger, C. and Einarsson, P.: Geophysical constraints on the dynamics of spreading centres from rifting episodes on land. *Nature Geoscience*, **5(4)**, (2012), 242-250.